Topological quantum well resonances in metal overlayers

Xiaoxiong Wang,[1,2,3,*] Guang Bian,[2,3] T. Miller,[2,3,4] and T.-C. Chiang[2,3,4,†]

[1]*College of Science, Nanjing University of Science and Technology, Nanjing 210094, China*

[2]*Department of Physics, University of Illinois at Urbana-Champaign, 1110 West Green Street, Urbana, Illinois 61801-3080, USA*

[3]*Frederick Seitz Materials Research Laboratory, University of Illinois at Urbana-Champaign, 104 South Goodwin Avenue, Urbana, Illinois 61801-2902, USA*

[4]*Synchrotron Radiation Center, University of Wisconsin-Madison, 3731 Schneider Drive, Stoughton, WI 53589-3097, USA*

(Received 19 December 2012; published 12 June 2013)

The electronic structure of thin Ca/Sr alloy films epitaxially grown on the topological insulator Bi_2Se_3 is investigated by first-principles calculations. Despite a negligible spin-orbit coupling in Ca/Sr alloys and strict spin degeneracy in freestanding Ca/Sr films, the topological surface states on the pristine Bi_2Se_3 surface are spatially transferred, upon Ca/Sr overlayer growth, into the overlayer to form topological quantum well resonances characterized by a spin-polarized chiral Dirac cone. The physical origin of this effect and the implications regarding applications are discussed.

DOI: 10.1103/PhysRevB.87.235113 PACS number(s): 73.20.−r, 71.70.Ej, 79.60.Dp

I. INTRODUCTION

Topological insulators[1–5] have unusual boundary properties arising from an inverted fundamental gap in the bulk. An ordinary (or trivial) insulator could be transformed into a topological insulator under increasing spin-orbit coupling, as illustrated schematically in Fig. 1(a), where the band gap becomes smaller, closes, and then reopens by anticrossing. Assuming the system is centrosymmetric, the resulting gap inversion is accompanied by parity reversal of the band edge states and a corresponding change in topological order. When a topological insulator is joined to an ordinary insulator to form a heterojunction, the gap must close at the boundary by analytic continuation,[6,7] as illustrated in Fig. 1(b). The resulting interface states must span the gap of the topological insulator and are spin-polarized by the Rashba interaction.[8,9] These topological interface states give rise to a metallic interface. In the ground state, they carry no charge current but a net transverse spin current at the Fermi level.[10–13] This unusual feature, being quite general and independent of the details of the interface, is of great interest for spintronic applications.[14,15] When the ordinary insulator involved in the heterojunction is an empty space or vacuum, the interface states reduce to the usual topological surface states that have been the subject matter of intense interest.

However, pristine surfaces of topological insulators are generally not suitable for applications; much more relevant to device architecture are heterojunctions. Of special interest, but thus far not well understood, are junctions between topological insulators and metals, which function as source and drain connections for spin and charge transport. Our study reported herein is a theoretical investigation of the electronic structure of a simple nonmagnetic metal overlayer on a topological insulator. Since metals must be topologically trivial (i.e., with an undefined topological order), it might appear that a metal overlayer would behave just as an ohmic contact with little influence on the spin structure of the system; however, we shall show that this is not the case, and the underlying physics is quite interesting.

The key idea is illustrated in Fig. 1(c). The inverted gap in the topological insulator must close at the interface with the metal overlayer and remain closed throughout the entire metal film before opening up at the metal-vacuum interface. The implication is that the topological interface states may now develop an extended spatial range where the gap is zero, as illustrated schematically in Fig. 1(c). Our study shows that this general picture is valid, but there are intricate details regarding the charge distribution, spin texture, and substrate-overlayer interaction. The extended states are actually quantum well resonances,[16] and they are topologically nontrivial and spin polarized *by inheritance*. The system chosen for our investigation is Ca/Sr alloy film epitaxially grown on the best-known topological insulator, Bi_2Se_3 (see Refs. 11 and 17). Alloys of Ca/Sr have a low atomic mass and negligible spin-orbit coupling. Their simple structure with space-inversion symmetry guarantees exact spin degeneracy for all states in freestanding films. Converting such simple metal films into topological conducting channels has strong implications for applications.

II. COMPUTATIONAL METHODS

Our calculations employed the ABINIT code,[18,19] Hartwigsen-Goedecker-Hutter pseudopotentials,[20] and a plane-wave basis within the local-density approximation (LDA). Both Ca and Sr belong to group IIA in the periodic table. In metallic form, both have a simple face-centered cubic structure. The (111) face of a 1:1 alloy has a lattice constant well matched to that of rhombohedral Bi_2Se_3(111). Thus, we choose this particular alloy composition for the present study. Since Ca and Sr have very similar electronic structures, their cores in the alloy are represented by the average pseudopotential of Ca and Sr. The model system consisted of periodic supercells, where each supercell included a vacuum gap of 15 Å and a slab made of a six quintuple-layer (QL) Bi_2Se_3 film symmetrically bracketed by various thicknesses of Ca/Sr films. The atomic structure, starting from the bare Bi_2Se_3 film to progressively thicker Ca/Sr overlayers, was optimized in each case by allowing the outermost six atomic layers to relax until the residual forces on the atoms became less than 2×10^{-5} hartree/bohr.

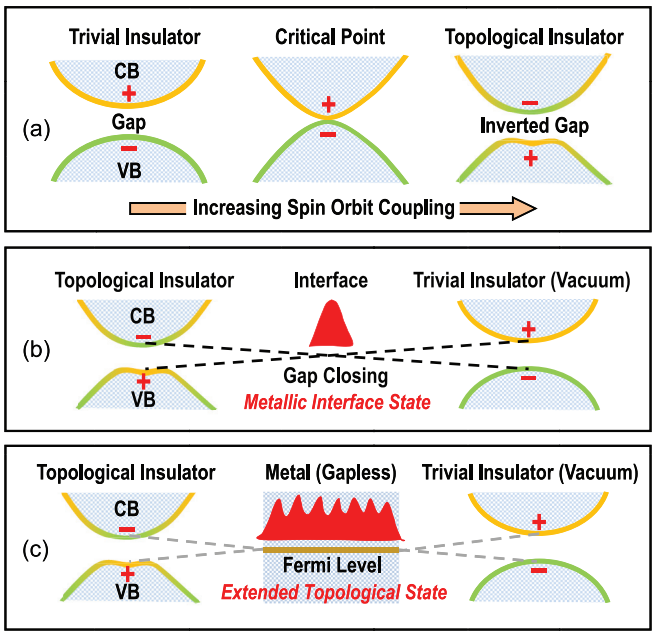

FIG. 1. (Color online) (a) Schematic transformation of an ordinary insulator into a topological insulator under increasing spin-orbit coupling, which can be realized experimentally by high-Z-element substitution. The abbreviations CB and VB denote the conduction and valence bands, respectively. The gap inversion is accompanied by parity reversal of the band edge states. (b) Illustration of the interfacial electronic structure at the junction between a topological insulator and an ordinary insulator. The gap must close at the junction, resulting in a metallic topological interface state, indicated by a red peak. (c) Similar to (b) but with the addition of a metal interlayer between the topological insulator and the ordinary insulator. The topological interface state is expected to stretch out to span the metal film.

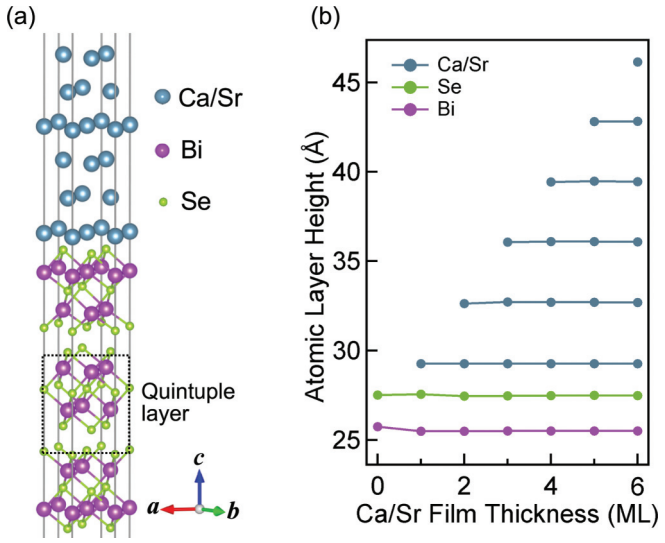

FIG. 2. (Color online) (a) Schematic atomic structure of a Bi_2Se_3 film with a six-ML Ca/Sr overlayer. (b) The heights of the top two atomic layers of Bi_2Se_3 and the Ca/Sr atomic layers, referenced to the midpoint of the six-QL Bi_2Se_3 substrate, as a function of overlayer thickness ranging from 0 to 6 MLs.

III. RESULTS AND DISCUSSION

The atomic configuration of a six monolayer (ML) Ca/Sr film on Bi_2Se_3 is shown in Fig. 2(a). The optimized atomic layer heights relative to the center of the Bi_2Se_3 slab as a function of the Ca/Sr overlayer thickness are shown in Fig. 2(b). The results indicate that structural relaxation effects are minimal. With just 1 ML of Ca/Sr adsorbed on the Bi_2Se_3 surface, each Ca/Sr atom resides in the threefold hollow site at 1.70 Å above the surface Se atoms. This distance is insensitive to the thickness of Ca/Sr overlayers. The overlayers at thicknesses greater than 1 ML adopt an essentially bulk Ca/Sr structure. The Bi_2Se_3 slab thickness chosen for the calculations, six QLs, is sufficiently large, so the topological surface states for the bare film are essentially in the bulk limit.[21,22]

Figure 3(a) shows the computed band structure of a freestanding six-QL Bi_2Se_3 film (curves), projected bulk band regions of Bi_2Se_3 (green regions), and the bulk fundamental gap (yellow region).[17] Surface and interface states can exist only within the bulk gap. We choose a coordinate system with $\hat{\mathbf{z}}$ along the surface normal and $\hat{\mathbf{x}}$ along the $\overline{\Gamma M}$ direction. Within the bulk gap are the gapless topological surface states that form a Dirac cone X at the zone center. The normalized spin polarizations

$$\sigma_y = \frac{1}{\hbar}\langle 2s_y \rangle \qquad (1)$$

of the surface states and their continuations as quantum-well states into the bulk band region (green regions) are indicated by the color coding. Near the zone center, the top branch is polarized along $-\hat{\mathbf{y}}$, while the lower branch is polarized along $+\hat{\mathbf{y}}$ for $k_x > 0$. The transverse spin texture reflects the chiral nature of the spin structure of Dirac cone X.[4,5] Away from the zone center, these gap-spanning surface states disperse into the projected bulk band regions, where they become quantum well states with diminishing net spin polarization (as indicated by the white color of the curves).[23]

Figure 3(c) presents the calculated band dispersion relations for a six-ML Ca/Sr overlayer on six-QL Bi_2Se_3. There are now two Dirac cones, Y and Z, within the bulk gap at the zone center. The color coding indicates the spin polarization. Dirac cone Z is adiabatically connected to Dirac cone X on the clean surface based on calculations in which the Ca/Sr film is moved gradually from far away into place on the Bi_2Se_3 substrate. Cone Y is derived from a pair of quantum well states Q originally localized within the Bi_2Se_3 substrate, dragged down by the interaction with the Ca/Sr film. Both cones Y and Z exhibit the same spin chirality. Since the states associated with Dirac cone Y are topologically trivial with both of its branches merging into the conduction band continuum, we shall focus on the topologically nontrivial Dirac cone, Z, only.

Figure 3(b) presents the band structure of a freestanding six-ML Ca/Sr film. All of the quantum well states are spin doublets with no net spin polarization (white color). Around the zone center, the quantum-well state doublet W and the topological surface state X of pristine Bi_2Se_3 are nearly degenerate. By bringing the Ca/Sr film and the Bi_2Se_3 slab together to form an interface, states W and X interact or hybridize to form the chiral states associated with Dirac cone Z. The topological order is preserved as there remains just one nontrivial Dirac cone at the zone center.

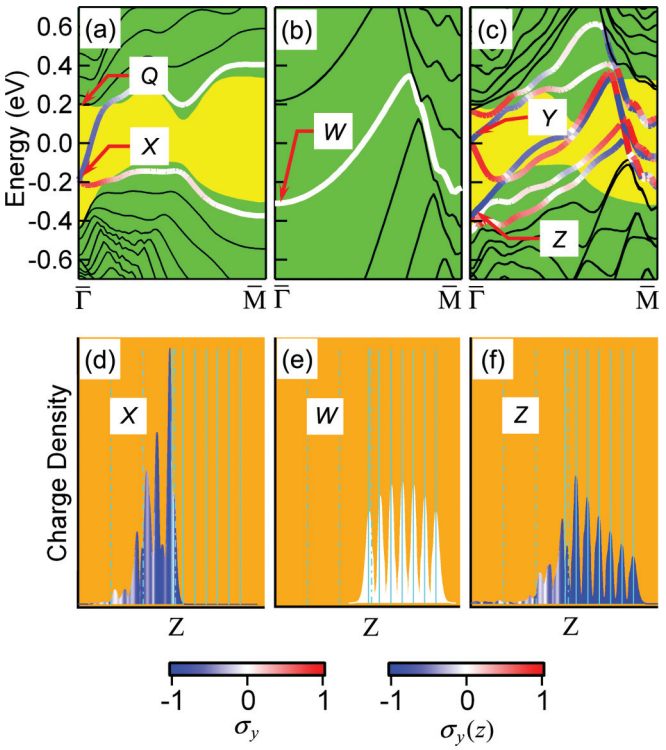

FIG. 3. (Color online) (a) Band structure of a six-QL freestanding Bi_2Se_3 film. The green and yellow regions indicate the bulk bands and the fundamental gap, respectively. The surface states within the gap form a Dirac cone, X, at the zone center. The color indicates the spin polarization σ_y. (b) Band structure of a freestanding six-ML Ca/Sr film. All bands are spin doublets. (c) Band structure of a six-QL Bi_2Se_3 film covered with a six-ML Ca/Sr film on each face. There are two Dirac cones, Y and Z. (d)–(f) The corresponding spin-polarized planar charge densities. The dashed and solid vertical lines mark the boundaries of Bi_2Se_3 QLs and Ca/Sr MLs, respectively. Each curve shows the z-dependent charge density, and the color filling indicates the z-dependent spin polarization $\sigma_y(z)$ of the upper state associated with the Dirac cone slightly offset from the zone center to avoid the spin degeneracy.

The nature of the states X, W, and Z is illustrated by the calculated spin-polarized planar charge densities presented in Figs. 3(d), 3(e), and 3(f), respectively, where the vertical dashed and solid lines indicate the boundaries of the QLs of Bi_2Se_3 and MLs of Ca/Sr. Each curve shows the z-dependent charge density, while the color filling under the curve indicates the z-dependent spin polarization

$$\sigma_y(z) = \frac{1}{\hbar}\langle 2s_y(z)\rangle \tag{2}$$

of the upper state associated with the Dirac cone slightly offset from the zone center to avoid the spin degeneracy. The topological state associated with cone X is mostly confined within the top QL of Bi_2Se_3 and spin-polarized along $-\hat{\mathbf{y}}$. The quantum-well states associated with W are exactly spin degenerate, as indicated by the white color, and they show the characteristic confined charge pattern of a quantum-well state. In the composite system, the topological state associated with cone Z has its charge mostly distributed within the film, where it is strongly spin polarized. It also has a weak tail in the substrate that resembles the pristine topological surface state of Bi_2Se_3 but with reduced spin polarization. The charge density within the film closely resembles that of the quantum-well state of the freestanding Ca/Sr film; the main differences are the strong spin polarization and a gradual decay away from the interface. The decay length of the charge density (wave function) is about 10 (20) MLs, a very large distance. The slow decay indicates a somewhat damped quantum-well state, or more precisely, a quantum-well resonance.

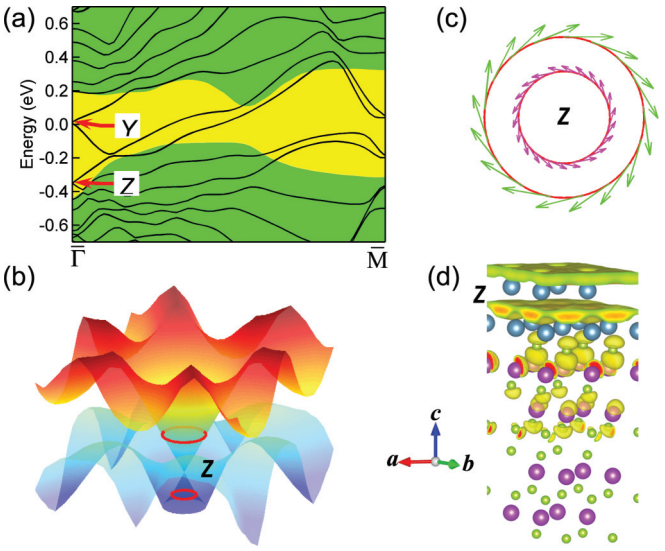

FIG. 4. (Color online) (a) Theoretical band structure of a six-QL Bi_2Se_3 slab capped by a two-ML Ca/Sr film on each face. The color shading indicates the bulk band gap as in Fig. 3. (b) The three-dimensional dispersion relations of Dirac cone Z near the zone center. The circles indicate two constant-energy cuts, one above the Dirac point (larger circle), and the other below (smaller circle). (c) The constant-energy contours corresponding to the two cuts. The arrows indicate the calculated directions of spin polarization. The chiral nature of the cone is evident. (d) The three-dimensional charge distribution of the upper branch of Dirac cone Z slightly offset from the zone center.

We have performed calculations for various Ca/Sr film thicknesses. The results confirm the general observation that the original topological surface states are transformed into topological quantum well resonances in the film. Figure 4(a) shows the theoretical band structure of a six-QL Bi_2Se_3 slab capped on both faces by two-ML Ca/Sr films. Despite the appearance of two Dirac cones at the zone center, the number of Fermi-level crossings within the gap between $\overline{\Gamma}$ and $\overline{M}$ is either three or five, an odd number consistent with the topological order. The three-dimensional dispersion relations of Dirac cone Z near the zone center are shown in Fig. 4(b). The circles indicate two constant-energy cuts, one above the Dirac point (larger circle) and the other below (smaller circle). The resulting constant-energy contours, shown in Fig. 4(c), are almost perfectly circular with negligible warping. The arrows indicate the calculated directions of spin polarization. The chiral nature of the Dirac cone is evident, with the two circles exhibiting opposite senses of chirality. Figure 4(d) shows the three-dimensional charge distribution of the upper branch of Dirac cone Z slightly offset from the zone center. Two nearly

uniform layers dominate the distribution: one above and the other in-between the 2 MLs of Ca/Sr. The distribution is mostly of the p_z character, and the charge distribution within the xy plane is characteristic of a metallic state.

The gradual decay in the film of the extended topological states (quantum well resonances) associated with cone Z in the composite system is an interesting finding that did not come out immediately in the general discussion related to Fig. 1. Yet it does not violate the topological constraints and can be understood as follows. Consider the limit of a very thick metal overlayer. Its electronic structure deep in the bulk part must be independent of the boundary condition. Specifically, there can be no spin texture. Any charge perturbation in a good metal is typically screened out within about a Debye length ($\sim$1 Å) because of strong Coulomb interactions between charges. By contrast, screening of spin texture is generally much less effective in simple metals. This explains the slow decay of the topological quantum well resonances.

IV. CONCLUDING REMARKS

Our findings suggest opportunities for new device engineering concepts based on these pseudotopological metal films. Defects such as steps and impurities on topological insulator surfaces can be a severe limiting factor for two-dimensional transport (while backscattering by nonmagnetic point defects is suppressed, side scattering and high-order effects are still problematic).[24,25] Such transport bottlenecks can be minimized or bypassed by spreading out the spin-conduction channel over the thickness of an overlayer. This thickness becomes an extra adjustable parameter, useful for optimizing device characteristics. It is also interesting to note that spin transport via topological surface states would likely involve metal contacts. How to preserve and transmit the spin polarization information across the interface is an important issue. Our results reveal a decay length of the topological quantum well resonances, which is long enough to fit well the usual nanoscale device architecture.

ACKNOWLEDGMENTS

This work was supported by the US Department of Energy, Office of Science (Grant DE-FG02-07ER46383 for TCC), the National Natural Science Foundation of China (No. 11204133 for XW), the Jiangsu Province Natural Science Foundation of China (No. BK2012393 for XW), and the Young Scholar Project of NUST. GB acknowledges partial support by the Yee Memorial Fund Fellowship.

*Corresponding author: phywangxx@njust.edu.cn
†tcchiang@illinois.edu

[1] C. L. Kane and E. J. Mele, Science **314**, 1692 (2006).
[2] M. König, S. Wiedmann, C. Brüne, A. Roth, H. Buhmann, L. W. Molenkamp, X.-L. Qi, and S.-C. Zhang, Science **318**, 766 (2007).
[3] J. E. Moore, Nature **464**, 194 (2010).
[4] M. Z. Hasan and C. L. Kane, Rev. Mod. Phys. **82**, 3045 (2010).
[5] X.-L. Qi and S.-C. Zhang, Rev. Mod. Phys. **83**, 1057 (2011).
[6] L. Fu, C. L. Kane, and E. J. Mele, Phys. Rev. Lett. **98**, 106803 (2007).
[7] L. Fu and C. L. Kane, Phys. Rev. B **76**, 045302 (2007).
[8] Z.-H. Zhu, G. Levy, B. Ludbrook, C. N. Veenstra, J. A. Rosen, R. Comin, D. Wong, P. Dosanjh, A. Ubaldini, P. Syers, N. P. Butch, J. Paglione, I. S. Elfimov, and A. Damascelli, Phys. Rev. Lett. **107**, 186405 (2011).
[9] P. D. C. King *et al.*, Phys. Rev. Lett. **107**, 096802 (2011).
[10] D. Hsieh, D. Qian, L. Wray, Y. Xia, Y. S. Hor, R. J. Cava, and M. Z. Hasan, Nature **452**, 970 (2008).
[11] Y. Xia, D. Qian, D. Hsieh, L. Wray, A. Pal, H. Lin, A. Bansil, D. Grauer, Y. S. Hor, R. J. Cava, and M. Z. Hasan, Nat. Phys. **5**, 398 (2009).
[12] D. Hsieh, Y. Xia, L. Wray, D. Qian, A. Pal, J. Dil, J. Osterwalder, F. Meier, G. Bihlmayer, C. Kane, Y. S. Hor, R. J. Cava, and M. Z. Hasan, Science **323**, 919 (2009).
[13] Y. L. Chen, J. G. Analytis, J. H. Chu, Z. K. Liu, S. K. Mo, X. L. Qi, H. J. Zhang, D. H. Lu, X. Dai, Z. Fang, S. C. Zhang, I. R. Fisher, Z. Hussain, and Z. X. Shen, Science **325**, 178 (2009).
[14] D. Pesin and A. H. MacDonald, Nat. Mater. **11**, 409 (2012).
[15] S. A. Wolf, D. D. Awschalom, R. A. Buhrman, J. M. Daughton, S. von Molnar, M. L. Roukes, A. Y. Chtchelkanova, and D. M. Treger, Science **294**, 1488 (2001).
[16] T. C. Chiang, Surf. Sci. Rep. **39**, 181 (2000).
[17] H. Zhang, C. X. Liu, X. L. Qi, X. Dai, Z. Fang, and S. C. Zhang, Nat. Phys. **5**, 438 (2009).
[18] X. Gonze *et al.*, Comput. Phys. Commun. **180**, 2582 (2009).
[19] X. Gonze *et al.*, Z. Kristallogr. **220**, 558 (2005).
[20] C. Hartwigsen, S. Goedecker, and J. Hutter, Phys. Rev. B **58**, 3641 (1998).
[21] Y. Zhang, K. He, C.-Z. Chang, C.-L. Song, L.-L. Wang, X. Chen, J.-F. Jia, Z. Fang, X. Dai, W.-Y. Shan, S.-Q. Shen, Q. Niu, X.-L. Qi, S.-C. Zhang, X.-C. Ma, and Q.-K. Xue, Nat. Phys. **6**, 584 (2010).
[22] O. V. Yazyev, J. E. Moore, and S. G. Louie, Phys. Rev. Lett. **105**, 266806 (2010).
[23] G. Bian, T. Miller, and T. C. Chiang, Phys. Rev. Lett. **107**, 036802 (2011).
[24] L. Fu, Phys. Rev. Lett. **103**, 266801 (2009).
[25] Z. Alpichshev, J. G. Analytis, J. H. Chu, I. R. Fisher, Y. L. Chen, Z. X. Shen, A. Fang, and A. Kapitulnik, Phys. Rev. Lett. **104**, 016401 (2010).